Valence of YbS under pressure: A resonant inelastic x-ray emission study

E. Annese,[1] J-P. Rueff,[2] G. Vankó,[3] M. Grioni,[4] L. Braicovich,[5] L. Degiorgi,[6] R. Gusmeroli,[7] and C. Dallera[5]
[1]*INFM - Dipartimento di Fisica, Università degli Studi di Modena e Reggio Emilia, via Campi 213/A, I-41100 Modena, Italy*
[2]*Laboratoire de Chimie Physique - Matière et Rayonnement (UMR 7614), Universitè Pierre et Marie Curie, 11 rue Pierre et Marie Curie, F-75231 Paris Cédex 05, France*
[3]*European Synchrotron Radiation Facility, B.P. 220, 38043 Grenoble Cédex, France*
[4]*IPN, Ecole Polytechnique Fédérale (EPFL), CH-1015 Lausanne, Switzerland*
[5]*INFM - Dipartimento di Fisica, Politecnico di Milano, piazza L. da Vinci 32, 20133 Milano, Italy*
[6]*Solid State Physics Laboratory, ETH-Zurich, CH-8093 Zurich, Switzerland*
[7]*Dipartimento di Elettronica e Informazione, Politecnico di Milano, piazza L. da Vinci 32, 20133 Milano, Italy*
(Received 29 February 2004; published 31 August 2004)

We present spectroscopic data on the electronic structure of YbS under pressure. From resonant x-ray emission and x-ray absorption spectra in the high-resolution partial fluorescence yield mode, we find that the Yb valence increases from 2.3 at ambient pressure to 2.6 at 360 kbar. The accuracy of these estimates is enhanced by a combined analysis of emission spectra measured as a function of the incident and emitted energy. The spectral line shapes reflect the mixed character of the electronic states, intermediate between atomic and bandlike.

DOI: 10.1103/PhysRevB.70.075117 PACS number(s): 78.70.Ck, 78.70.Dm, 71.27.+a, 71.30.+h

I. INTRODUCTION

Rare earth (RE) monochalcogenides, like many RE-based materials, exhibit interesting physical phenomena associated with the partially filled $4f$ orbitals. In particular, the Sm, Tm, and Yb monochalcogenides undergo semiconductor-metal transitions,[1] associated with valence changes. It has been suggested that at the transition a $4f$ electron is promoted into the $5d$ conduction band, following the pressure-induced reduction of their energy separation.[2] Theory confirms that, for sufficiently high pressures, the trivalent configurations of the RE ions are thermodynamically more stable than the divalent ones.[3,4] Transition pressure values have been estimated by *ab initio* calculations combining an atomic-like description of the f electrons with an itinerant description of the other electronic degrees of freedom.[5] A complete description of these systems should also take into account the possibility of intermediate-valent (IV) ground states, and of noninteger changes in the $4f$ population. However, this complex theoretical problem is far from being solved. Moreover, direct experimental knowledge of the $4f$ occupation under pressure is scarce.

Yb monochalcogenides are characterized by the high stability of the divalent (Yb^{2+}) $4f^{14}$ configuration, expressed by larger (by $\sim$1.5 eV) values of the third ionization potential relative to the corresponding Sm and Tm cases. Therefore, whereas moderate pressures ($p<50$ kbar) are enough to reach an IV ground state in Sm and Tm compounds, several hundreds of kilobars are needed for the Yb monochalcogenides.[6–9] The variation of $4f$ occupation is reflected in the pressure dependence of the lattice constants, due to the substantially smaller size of the trivalent ion. YbS, which does not exhibit the NaCl to CsCl structural change of other RE monochalcogenides, is an especially clear case. Compressibility data[6,10] show that the experimental pressure violating (PV) relation is intermediate between those of the Yb^{2+} and Yb^{3+} configurations, and suggest a rearrangement of the electronic structure in the 150–200 kbar range. This interpretation is supported by self-interaction corrected-local spin density (SIC-LSD) calculations, which points to a valence instability in YbS around 75 kbar.[5] At 300 kbar the specific volume of YbS is half-way between the divalent and trivalent reference curves, indicating that the Yb valence is still far from 3. A lattice parameter scaling yields $v=2.4$ at 250 kbar, but the uncertainty is rather large (± 0.15), because reference volume values are not well established at high pressures.

Spectroscopic data of the $4f$ occupation under pressure is rather scarce. The optical reflectivity spectrum of YbS shows a pronounced edge close to 1 eV. This feature, characteristic of the Yb ion only, was interpreted as an excitation of $d \rightarrow f$ character.[10] Pressure shifts the absorption band to lower energies. The measured optical $4f-5d$ gap ($\sim$1 eV) and its decrease rate with pressure suggests the onset of f-d energy overlap (and the consequent valence change) near 100 kbar and the closure of the gap near 200 kbar The semiconductor-metal transition is confirmed by a change of color, from black to golden yellow above 200 kbar.

The Yb valence in YbS has also been studied by x-ray absorption (XAS) at the Yb $L_{2,3}$ edges. The XAS process is element specific and probes the local $5d$-like configuration at the Yb site. In Ref. 11 the valence of YbS was estimated to increase from $\sim$2 at ambient pressure to $\sim$2.5 at 300 kbar by analyzing the change of the Yb L_3 absorption line shape. An accurate determination of valence from absorption data is however hindered by the broad line shapes which reflect the short lifetime of the final excited state.

Recent advances in synchrotron radiation spectroscopies have opened possibilities to circumvent this problem. We present here results on the electronic structure of YbS between ambient pressure and 360 kbar. We performed Yb L_3 XAS measurements in the high-resolution partial fluores-

cence yield (PFY) mode, and resonant x-ray emission (RXES) measurements as a function of incident and emitted photon energy. These techniques are well suited to study the pressure and temperature induced valence change in Yb material, because of the bulk sensitivity and the resonant enhancement, as previously shown in metallic IV Yb materials such as $YbAgCu_4$ and $YbAl_2$.[12,13] We extend here the analysis to a more ionic, insulating compound.

II. EXPERIMENT

The YbS single crystals were prepared via elemental synthesis. Sulfur was obtained by cracking H_2S gas at 600–700 °C. Stoichiometric amounts of metal and sulfur weighted to the nearest of 5 mg, in batches of approximately 0.1 mole, were introduced into a fused alumina crucible contained in a quartz tube. The tube was then sealed off under vacuum and heated first to 500–600 °C until all sulfur vapors disappeared, then to 800–900 °C for 5–6 h. The samples were then sintered in purified argon at 1500–1600 °C.

The sample was optically characterized by reflectivity measurements performed over a spectral range extending from the far infrared up to the ultraviolet. Our spectra agree with previous data.[2,9,10] This confirms the good quality of the samples. Besides the strong phonon modes in the far infrared spectral range, the optical spectra display several absorptions above 1 eV, ascribed to electronic interband transitions. The onset of the gap, coinciding with the $4f$-$5d\ t_{2g}$ transition, is at $\sim$1 eV. The final multiplet states of the $4f^{14}$-$4f^{13}5d\ (t_{2g}, e_g)$ transitions lead to absorption features between 2 and 10 eV.

X-ray measurements were performed at beamline ID16 at the European Synchrotron Radiation Facility (ESRF). The beamline is equipped with a fixed-exit Si(111) monochromator and a toroidal focusing mirror providing a $130 \times 50\ \mu m^2$ (H×V) beam spot at the sample position. The samples were crushed into powder and loaded in a diamond anvil cell along with ruby chips, using high-strength Be as gasketting material. Pressure values were measured *in situ* by a conventional ruby fluorescence technique. The experiment was performed in radial geometry, i.e., both the incident and scattered radiation passed through the Be gasket, in order to avoid the strong absorption by the diamonds. The intensity loss through the pressure cell was estimated at about one order of magnitude. The emitted beam was analyzed by a 1 -m radius spherically-bent Si(620) crystal and detected by a Peltier-cooled Si diode. The total experimental resolution was $\sim$1.5 eV The acquisition time for the PFY spectra was $\sim$15 min. For the RXES spectra it varied between $\sim$15 and $\sim$25 min, depending on the incident energy. The count rate under pressure was $\sim$500 cps on the peak with excitation at the Yb^{2+} resonance. All data were collected at room temperature.

III. RESULTS AND DISCUSSION

The $L\alpha_1$ PFY spectra of YbS were obtained by recording the intensity of the Yb $2p^5 4f^n \epsilon d \rightarrow 3d^9 4f^n \epsilon d$ decay channel (ϵd is the electron added to a continuum state of d character) as a function of incident energy at the Yb L_3 edge. We collected photons in a 1 eV energy window around $h\nu_0 = 7.415$ keV, which corresponds to the maximum of the fluorescent $L\alpha_1$ emission (i.e., following excitation well above the L_3 threshold). This reduces the intrinsic spectral broadening with respect to a traditional L_3 XAS experiment, from $\sim$4.5 to $\sim$1.5 eV, as determined by the lifetime of the $2p$ and $3d$ final state core-hole, respectively.[14] It has been shown[15] that PFY spectra do not strictly coincide with absorption spectra deconvoluted by their final state lifetime. However the better contrast is of great help in evaluating the relative intensity of the divalent and trivalent spectral features, which are representative of the valence changes. PFY spectra of YbS measured up to 360 kbar (Fig. 1) exhibit two structures at $\sim$8.946 and 8.952 keV in the L_3 edge region. These features correspond to transitions from the Yb^{2+} and Yb^{3+} components of the mixed valent ground state ($|\Psi_0\rangle = a|4f^{13}\rangle + b|4f^{14}\rangle$). The Coulomb interaction between the "spectator" $4f$ hole and the $3d$ core hole in the excited final state separates the two continua $3d^9 4f^{14} \epsilon d$ and $3d^9 4f^{13} \epsilon d$ by $\sim$6 eV. The intensity ratio of the two peaks decreases with pressure.

A quantitative estimate of the valence change in YbS can be obtained by decomposing each PFY spectrum in its 2+ and 3+ contributions. We modeled the spectrum by the superposition of two phenomenological lineshapes shifted by $\sim$6 eV. In order to reproduce the sharp edge and the continuum region of the spectrum, each line shape was the sum of a Gaussian and an error function. Best results were obtained by assigning a different Gaussian width for the divalent [full width at half maximum (FWHM)=4 eV] and trivalent component (FWHM =7 eV), while the width of the error function was kept at a constant value of 1.5 eV, corresponding to the lifetime broadening of the $3d \rightarrow 2p$ decay channel. We impose that the sharp edge inflection point be located at the center of the Gaussian profile. PFY spectra at different pressures were then fitted by changing only the relative intensities of the two line shapes. The typical quality of the fit is illustrated in the lower panel of Fig. 1. This analysis does not account for a weak preedge shoulder (vertical arrow), which we attribute to $2p \rightarrow 4f$ quadrupolar transitions. Such transitions are dipole-forbidden, and are possible only from the trivalent $4f^{13}$ configuration. The intensity ratio of the electric-quadrupolar to the electric-dipolar trivalent component is constant ($\sim$0.04) for all spectra, which supports our interpretation. The Yb valence v was evaluated as $v = 2 + I^{3+}/(I^{2+} + I^{3+})$ where I^{2+} and I^{3+} are the integrated intensity of the 2+ and 3+ components. The values are reported in Fig. 6 (circles).

Because we consider an inelastic emission channel, here, as well as for our RIXS data, reabsorption effects on the outgoing path for the 2+ and 3+ peaks can be neglected. The (nonresonant) absorption of the two signals in fact only differs by $\sim$0.1%, and our valence estimates would be affected by much less than their error bar.

Figure 1 also shows the result of a convolution of the PFY spectrum at ambient pressure by a Lorentzian line shape with FWHM =4.5 eV (the lifetime width of the $2p_{3/2}$ core-hole) to simulate a conventional XAS spectrum.[16] Clearly, the broad line shape makes the evaluation of the relative intensity of

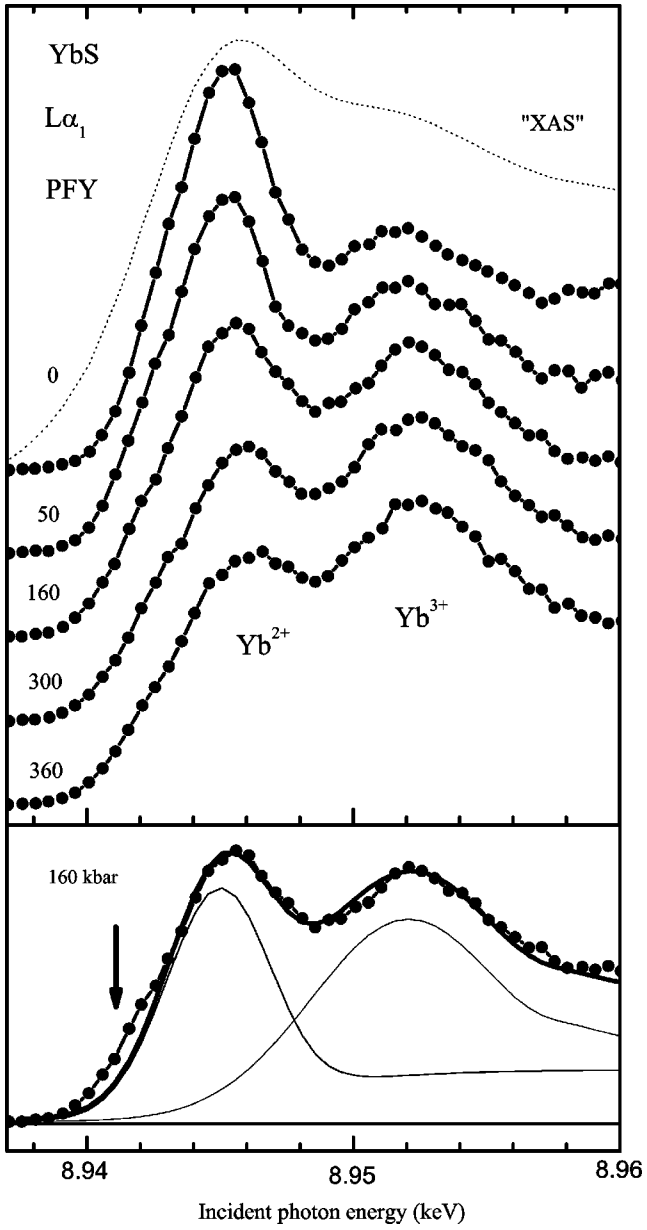

FIG. 1. Upper panel: Yb L_3 PFY spectra of YbS measured at pressures between 0 and 360 kbar (given on the left), showing the progressive transfer of spectral weight from 2+ to 3+ components. The thin dotted spectrum simulates a "normal" XAS spectrum and is obtained by convoluting the upper spectrum with the L_3 XAS final state lifetime. Lower panel: Decomposition of the PFY spectrum at $p=160$ kbar (dots) into the divalent and trivalent components (thin solid lines). The thick solid line is the sum of the two fitting components. The arrow points to the quadrupolar pre-edge feature.

Yb^{2+} and Yb^{3+} rather arbitrary. It would also mask possible differences in the spectral components.

In a previous analysis of PFY spectra of $YbAl_2$ we have used identical line shapes for Yb^{2+} and Yb^{3+},[13] consistent with the XAS literature on IV Yb intermetallics.[17] That choice would not be possible here. In order to confirm this, we performed calculations of the XAS final state multiplets for both Yb configurations, which clarifies the origin of the

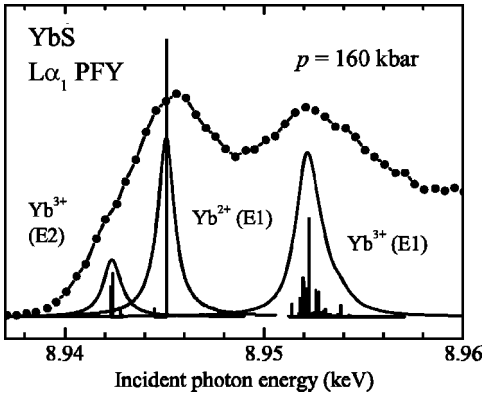

FIG. 2. Calculation of the atomic multiplet of the $2p \rightarrow 5d$ transition for two different ground state configurations $2p^6 4f^{14}$ (Yb^{2+}) and $2p^6 4f^{13} 5d^1$ (Yb^{3+}). Dipolar ($E1$) and quadrupolar ($E2$) transitions were calculated with Cowan's code (see text for details).

different widths, and suggests an explanation for this discrepancy. The results of the atomic calculation, for which we used Cowan's code,[18] are shown in Fig. 2. The ground state configurations were $2p^6 4f^{14} 5d^0$ (Yb^{2+}) and $2p^6 4f^{13} 5d^1$ (Yb^{3+}), and the usual rescaling of the Slater integrals to 80% of their Hartree-Fock value was applied to account for intra-atomic screening effects. Dipolar ($E1$) transitions were calculated for both configurations, and the quadrupolar ($E2$) transition for Yb^{3+}. The $E1$ multiplets for Yb^{2+} and Yb^{3+} consist of, respectively, 2 and 68 lines, the $E2$ multiplet consists of 8 lines. The multiplet were convoluted with a Lorentzian line shape with FWHM =1.5 eV, corresponding to the lifetime of the $3d$ core-hole in the PFY final state, and all calculated curves were rescaled by arbitrary factors to ease visual comparison with the experimental spectrum. The atomic calculation cannot reproduce the measured spectral shape but provides important information on the energy distribution of the multiplets. Namely, it indicates that the energy width of the Yb^{3+} PFY peak is due to the larger spread of the final state multiplet, thus providing a rationale for the different phenomenological line shapes of Fig. 1. Of course, in a more realistic calculation each final state would acquire an energy width of the order of the conduction bandwidth. Such broadening would largely dominate the spectrum of metallic materials having a broad band [almost 15 eV wide (Ref. 19)], like $YbAl_2$. On the contrary, the fingerprint of the underlying atomic multiplet remains visible in more ionic materials with narrower bands, like YbS, where the $5d$ band extends over $\sim$6 eV.

A further, similarly accurate determination of the Yb valence may be obtained by RXES. The RXES experiment consists here of measuring the emission spectra corresponding to the decay of the excited state to final states where the $2p_{3/2}$ hole was filled by a $3d_{5/2}$ electron ($h\nu_{\mathrm{OUT}} \sim 7.4$ keV), after a primary resonant excitation of a Yb $2p$ electron (as in Yb L_3 XAS). In the RXES final state the Coulomb interaction due to the $3d$ core-hole splits the divalent and trivalent spectral features, similarly to XAS. Moreover, because of the resonant process, the 2+ and 3+ configurations can be separately enhanced, depending on the incident energy. Thus, the evolution of the spectral shape as a function of the excitation

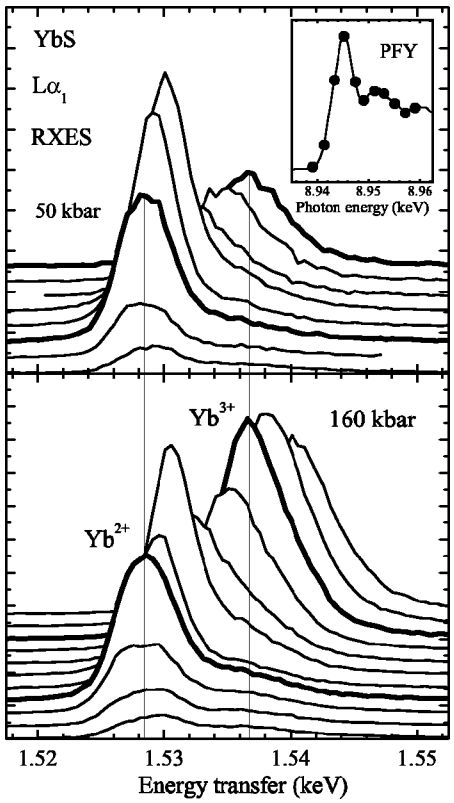

FIG. 3. Yb Lα_1 RXES spectra measured at 50 and 160 kbar at 2 eV incident energy steps. The spectra corresponding to the maxima of the 2+ and 3+ resonance profiles are highlighted (thick solid line). The incident energies are indicated by the dots on the PFY spectrum at ambient pressure (inset).

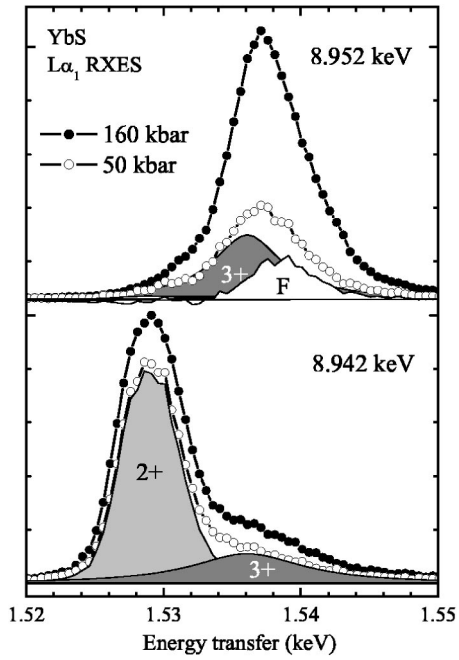

FIG. 4. $L\alpha_1$ RXES spectra measured at 160 kbar (black dots) and 50 kbar (white dots) at incident energies corresponding to the divalent and trivalent resonance of Yb ($h\nu_{IN}$=8.942 keV and $h\nu_{IN}$ =8.952 keV, respectively). The spectra are decomposed in their divalent component (light gray), trivalent component (dark gray), and fluorescence component (white).

energy and its change with pressure provide information on the Yb electronic configuration.

For each pressure point indicated in Fig. 1, RXES spectra were measured at various excitation energies $h\nu_{IN}$ along the L_3 absorption edge. Figure 3 shows representative RXES spectra at 50 and 160 kbar, plotted as a function of the transferred energy ($h\nu_T = h\nu_{IN} - h\nu_{OUT}$). Emission features with Yb^{2+} and Yb^{3+} character are identified at $h\nu_{T_2}$=1.529 keV±0.5 eV and $h\nu_{T_3}$=1.535±0.5eV, as indicated by the thin vertical lines. The incident energies at which the resonances occur do not coincide with the maxima of the 2+ and 3+ peaks in the PFY spectrum, where the spectral energies arise from a combination of intermediate and final states. The valence variation versus pressure is evident from the changes in the relative weight of the divalent and trivalent peaks. At 50 kbar the spectral intensity at large $h\nu_T$ and $h\nu_{IN}$ mainly comes from fluorescent emission from Yb^{2+}. Valence changes were determined by decomposing the RXES spectra, and evaluating the integrated RXES intensity of Yb^{2+} and Yb^{3+} at the maximum of their respective resonance profiles. The procedure follows that of $YbAl_2$ in Ref. 13, but the line shapes are different, reflecting the more ionic character of YbS. Examples of decomposition are given in Fig. 4, for p=50 and 160 kbar. Spectra excited below the Yb^{2+} resonance were fitted first, since they only require two components. The Yb^{3+} line shape is phenomenologically modeled by a Lorentzian whose intensity and width are optimized by fitting the high energy-transfer side of each spectrum. We find that the width changes as a function of $h\nu_{IN}$ from 10 to 5 eV, due to the resonant narrowing typical of the second order emission process. The Yb^{2+} line shape does not exhibit a similar narrowing, because the incident energy does not span a comparable range below threshold. The divalent line shape is obtained by subtraction of the Yb^{3+} signal. Beyond the Yb^{2+} resonance the fit requires an additional component describing normal fluorescence. The divalent weight rapidly vanishes, the trivalent intensity is scaled to match the leading edge of the spectrum with the constraint that the peak position of the fluorescent contribution, obtained by subtracting from the spectra the line shapes of Yb^{2+} and Yb^{3+}, must be constant versus $h\nu_{OUT}$. The valence values obtained by this procedure are reported in Fig. 6 (triangles).

A separate analysis of RXES spectra excited well below the absorption threshold ($h\nu_{IN}$=8.936 keV) yields an independent estimate of the Yb valence. In this case the absence of the fluorescent contribution simplifies the analysis (see Fig. 5). When all spectra are normalized to the same height of the divalent peak, the intensity of the trivalent feature is an indicator of valence changes. We used a Gaussian profile for Yb^{2+} and obtained the line shape of Yb^{3+} by subtracting the divalent part from the spectrum at ambient pressure. Fits of the spectra at all pressures were performed adjusting the intensity of the trivalent signal.[20]

The lower panel of Fig. 5 displays the emission spectra for Yb^{3+} and Yb^{2+} from the Kramers-Heisenberg formula, with atomic cross sections calculated by Cowan's code. The experimental spectrum at ambient pressure is displayed in

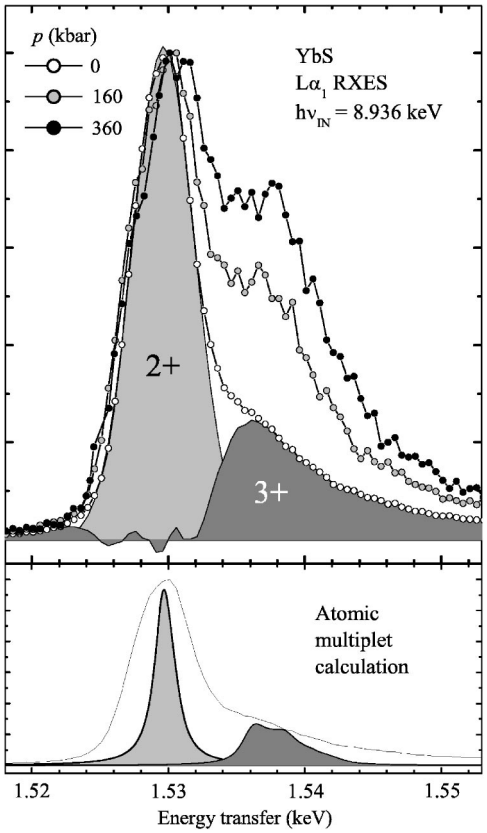

FIG. 5. Upper panel: pressure dependent RXES spectra excited below the absorption threshold ($h\nu_{IN}$=8.936 keV) The evolution of the 3+ component follows the valence increase with pressure. The decomposition of the spectrum at ambient pressure into 2+ (light gray) and 3+ (dark gray) contributions is given. Lower panel: emission spectra calculated in the atomic model. The spectrum at ambient pressure (thin line) is repeated for comparison.

the same panel (thin line). The asymmetric line shape of Yb^{3+} shows a remarkable resemblance with the result of the fit. The calculated atomic Yb^{2+} line shape is much narrower than the measured one, which is affected by the bandwidth of the 5*d* states. The energy spread of the Yb^{3+} atomic multiplet is so large that the effect of the extended states is much less visible.

Figure 6 summarizes the various estimates of the Yb valence values from the present work. The spread of the extracted values is representative of the residual uncertainties in the estimate (less than ±0.5). Our data show differences from values extracted from XAS (Ref. 11), namely, a larger valence (~2.3 versus ~2) at ambient pressure. Given the bulk-sensitivity of the technique, the effect of a possible

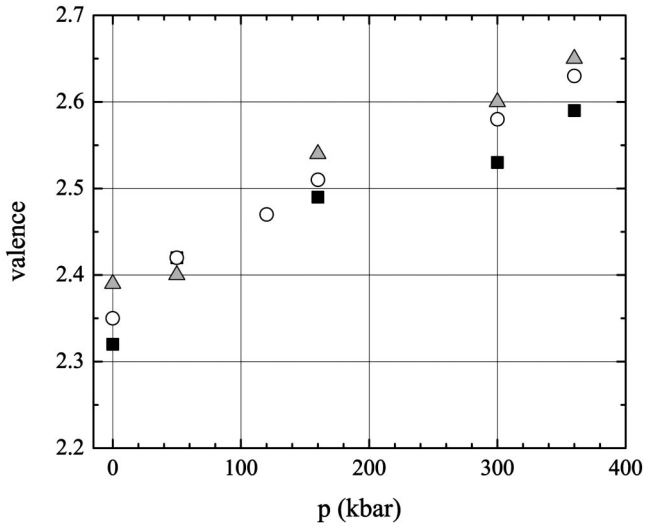

FIG. 6. Valence of ytterbium in YbS as a function of the applied pressure, obtained from the analysis as described in the text: PFY spectra (circles), RXES spectra versus $h\nu_{IN}$ (triangles), RXES spectra at $h\nu_{IN}$=8.936 keV (squares).

surface contamination from trivalent Yb_2O_3 should be negligible, especially in the measurements at ambient pressure which were performed on an intact single crystal sample. It seems likely instead that the accuracy of the previous estimates from L_3 XAS measurements could suffer from the broad line shapes. The valence variation we measure (~0.3) fully agrees with the theoretical prediction of Ref. 5, although with a clear discrepancy on the ambient pressure value, which we find to be larger than calculated.

IV. CONCLUSION

In summary, we have measured partial fluorescent yield and resonant x-ray emission spectra of YbS under pressure up to 360 kbar. These spectroscopic techniques have access to the electronic configuration and are therefore direct and highly sensitive probes of the valence state. We observe large changes in the valence, but even at the highest reached pressure the transition toward trivalency is far from complete. The hybridization between the 4*f* states and the 5*d* band increases under pressure, and leads to a gradual change from the metallic to the insulating state.

ACKNOWLEDGMENTS

C.D. wishes to thank P. Ferriani and C. M. Bertoni for invaluable support in the use of Cowan's codes.

[1] A. Chatterjee, A. K. Singh, and A. Jayaraman, Phys. Rev. B **6**, 2285 (1972).

[2] P. Wachter, in *Handbook on the Physics and Chemistry of Rare Earths*, Vol 19, edited by K. A. Gschneidner, L. Eyring, G. H. Lander, and G. R. Choppin (North-Holland, Amsterdam, 1994), Chap. 132, p. 177.

[3] B. Johansson, Phys. Rev. B **12**, 3253 (1975).

[4] A. Jayaraman, in *Handbook on the Physics and Chemistry of Rare Earths*, Vol 2, edited by K. A. Gschneider and L. Eyring (North-Holland, Amsterdam, 1979), p. 575.

[5] W. M. Temmerman, Z. Szotek, A. Svane, P. Strange, H. Winter, A. Delin, B. Johansson, O. Eriksson, L. Fast and J. M. Wills, Phys. Rev. Lett. **83**, 3900 (1999).
[6] A. Jayaraman, A. K. Singh, A. Chatterjee, and S. U. Devi, Phys. Rev. B **9**, 2513 (1974).
[7] A. Werner, H. D. Hochheimer, A. Jayaraman, and J. M. Leger, Solid State Commun. **38**, 325 (1981).
[8] H. G. Zimmer, K. Takemura, K. Syassen, and K. Fischer, Phys. Rev. B **29**, 2350 (1984).
[9] K. Syassen, J. Phys. (Paris), Colloq. **45**, C8-123 (1984).
[10] K. Syassen, H. Winzen, H. G. Zimmer, H. Tups, and J. M. Leger, Phys. Rev. B **32**, 8246 (1985).
[11] K. Syassen, Physica B & C **139-140**, 277 (1986).
[12] C. Dallera, M. Grioni, A. Shukla, G. Vankó, J. L. Sarrao, J. P. Rueff, and D. L. Cox, Phys. Rev. Lett. **88**, 196403 (2002).
[13] C. Dallera, E. Annese, J. P. Rueff, A. Palenzona, G. Vankó, L. Braicovich, A. Shukla, and M. Grioni, Phys. Rev. B **68**, 245114 (2003).
[14] K. Hämäläinen, D. P. Siddons, J. B. Hastings, and L. E. Berman, Phys. Rev. Lett. **67**, 2850 (1991).
[15] P. W. Loeffen, R. F. Pettifer, S. Müllender, M. A. van Veenendaal, J. Röhler, and D. S. Silvia, Phys. Rev. B **54**, 14 877 (1996).
[16] Due to technical difficulties in the presence of the pressure cell we could not measure conventional XAS. To our knowledge L_3 XAS spectra are not present in literature (only the valence values extracted from XAS spectra are shown in the paper of Ref. 11).
[17] A. L. Cornelius, J. M. Lawrence, J. L. Sarrao, Z. Fisk, M. F. Hundley, G. H. Kwei, J. D. Thompson, C. H. Booth, and F. Bridges, Phys. Rev. B **56**, 7993 (1997).
[18] R. D. Cowan, *The Theory of Atomic Structure and Spectra* (University of California Press, Berkeley, 1981).
[19] S. J. Lee, S. Y. Hong, I. R. Fisher, P. C. Canfield, B. N. Harmon, and D. W. Lynch, Phys. Rev. B **61**, 10 076 (2000).
[20] Note that the different distance between $h\nu_{\mathrm{IN}}=8.936$ keV and the energy of the 2+ and 3+ resonances is compensated by the different width of the resonance profiles.